Discrete Structural Models and Their Application To Gas-Solid Reacting Systems

Discrete models are developed to simulate the reaction of solids with complex pore structures in the kinetic- and diffusion-controlled regimes. Simulations employ two- and three-dimensional computational grids, and model parameters are directly obtainable from measurable physical properties of the unreacted solid. Model predictions can be displayed pictorially, allowing for direct visualization of the simulated process, while image processing of the computational grids can provide detailed structural information not easily obtainable from other analytical models. The effects of various pore structural parameters on the predicted reactivity patterns are investigated. Several examples are presented to illustrate the use of the models and demonstrate the significance of the pore structure in determining the reactivity of coal-derived chars.

Kyriacos Zygourakis
Charles W. Sandmann, Jr.
Department of Chemical Engineering
Rice University
Houston, TX 77251

Introduction

Gas-solid reactions are encountered in a wide variety of processes, such as the gasification and combustion of coal chars, activation of carbonaceous materials used for selective adsorption or separation applications, reaction of coke in ore processing, and others. All these reacting systems are characterized by continuous changes of the pore structure and reactivity of the solid reactant. Two competing phenomena determine the evolution of the pore structure: pore growth, and coalescence of neighboring pores. Pore enlargement is prominent at low conversions, resulting in increases of the surface area and the observed reaction rate. As pores grow, however, they coalesce with adjacent enlarging pores, causing the surface area and rate to decrease. Thus, rate vs. conversion curves may exhibit maxima or may decrease monotonically with conversion when pore coalescence dominates from the early stages of reaction.

The temporal evolution of the pore structure complicates the determination of intrinsic reaction rates that are necessary for the analysis and optimal design of commercial processes. In the kinetic control regime, the rate R can be expressed in the following simplified form

$$R = \frac{dx}{dt} = A(x)\, S_g(x)\, f(c_i, T) \qquad (1)$$

where x is the solid reactant conversion, $A(x)\, S_g(x)$ is the active pore surface area, $S_g(x)$ is the total pore surface area, and $f(T, c_i)$ is the expression yielding the intrinsic reaction rate dependent only on the gaseous reactant concentrations and temperature. If the reaction is carried out under constant temperature and reactant concentration conditions, the observable rate $R(x)$ will depend only upon the active surface area $A(x)\, S_g(x)$ of the sample. Under the additional assumption of a uniformly reactive surface, the observed reactivity and its evolution with conversion depends solely upon the total pore surface area $S_g(x)$.

If the temporal evolution of the total pore surface area S_g can be accurately predicted by a structural model, a comparison of theoretical predictions and observed reaction rates will provide the intrinsic reaction rates for systems with uniform and constant surface activity. Intraparticle diffusional limitations can then be included in a detailed model to accurately predict reaction rates under actual operating conditions. We should note here the limitations of this approach. The concentration of active sites per unit surface area may vary with conversion (Sandmann and Zygourakis, 1987), while solid additives or impurities may catalyze or hinder the reaction. The importance of such effects must be evaluated for each reacting system.

Perlmutter and coworkers (Bhatia and Perlmutter, 1980, 1981; Su and Perlmutter, 1985) developed a random-pore model describing the pore structure of the unreacted solid with two parameters obtainable from standard structural measurements. Gavalas (1980) followed a similar approach to develop an essen-

Correspondence concerning this paper should be addressed to K. Zygourakis.
The current address of C. W. Sandmann, Jr. is Shell Oil Company, Westhollow Research Center, Houston, TX 77001.

tially identical random capillary model also employing two parameters that can be obtained either by fitting reactivity data or from structural measurements. These models are easy to use and can accurately predict the reactivity pattern of several coal-derived chars, but are unable to satisfactorily simulate the gasification behavior of some chars with complex pore structure and reactivity patterns. For example, Ballal and Zygourakis (1987b) established that submicropores should be considered separately from the other pores, since their surface area may not be fully utilized during reaction. These and other experimental studies demonstrated the need for models sensitive to the complex bimodal pore structures characterizing many coal-derived chars. The random-pore models developed by Ballal and Zygourakis (1987a) met some of these requirements since they handled bimodal pore size distributions by employing four parameters obtained directly from experimental structural measurements. These models could treat pores with various shapes, as well.

Analytical models, however, cannot easily handle solids with complex pore structures and simplifications are necessary (Ballal and Zygourakis, 1987a) in order to obtain a tractable set of equations. Also, all the above models have not considered in detail the problems of initially closed porosity and of diffusional limitations in the continuously changing pore structure. An equivalent continuum approach is usually employed to treat the reaction-diffusion problem in such gas-solid systems. However, equivalent continuum assumptions may not be appropriate for the pore structures of interest here. Percolation models (Mohanty et al., 1982) could in principle simulate the combustion of a porous solid with closed porosity in the presence of diffusional limitations. However, coal chars may exhibit complex bimodal or even trimodal pore size distributions and the use of a single length scale (as is commonly done in percolation models) would give unsatisfactory predictions for the gasification behavior of structures with pore sizes ranging over several orders of magnitude. Finally, an additional complexity is introduced when one considers the substantial particle fragmentation occurring for conversions higher than 50%.

The development of novel structural models predicting the evolution of pore structure and surface area of solid reactants is the objective of this communication. A discrete simulation approach is described and its validity is established via a series of detailed parametric studies. Several model variants are presented whose parameters are obtained from measurable structural properties of the unreacted porous solids. These models are then used to analyze experimental reactivity data obtained by gasifying carbonaceous materials.

Development of the Discrete Models

Reactions of solids with complex pore structures are simulated on computational grids consisting of a large number of cells arranged in square or cubic lattices (Sandmann and Zygourakis, 1986). In the simplest case, each cell can represent either a solid or a pore volume element. Clusters of several adjacent cells with the same state define entities that model pores or solid grains with any dimension or shape. The simulations presented here employe entities approximating regular geometric objects (cylinders with various cross-sectional geometries and/or spheres). The geometric centers of these entities are randomly distributed in a cube assumed to be a representative unit of the porous solid reactant. Since these entities overlap, the resulting model solid has a network of pores with different irregular cross-sectional shapes and a distribution of sizes. The simplest models considered here assume that the pores are parallel overlapping cylinders with uniform or varying radius. In this case, the three-dimensional problem of distributing the pores in a cube reduces to a two-dimensional problem of distributing circles (or other two-dimensional entities corresponding to pore cross sections) on a face of the cube. The most complex models consider overlapping spheres and cylinders with random orientations and nonuniform size. As discussed below, the number and size of pores (or solid grains) distributed on the initial grids are calculated from measurable structural properties of the actual solids (porosities, surface areas, etc.)

Computational grids with two-state cells can be graphically displayed by using black to represent a void element and white to represent a solid element. For example, the image of Figure 1a can be visualized as a cross section of a porous solid with parallel cylindrical pores. This grid models the micropore structure of an Illinois No. 6 char and was generated by randomly distributing circles of uniform size on a 2,048 × 2,048 computational grid. By applying image analysis techniques on the image of Figure 1a, the narrow unimodal pore size distribution shown in Figure 1b was obtained. Figure 2a shows another 2,048 × 2,048 grid generated by randomly distributing circles whose diameters followed a unimodal probability density function. Note that the two micropore structure realizations of Figures 1a and 2a have

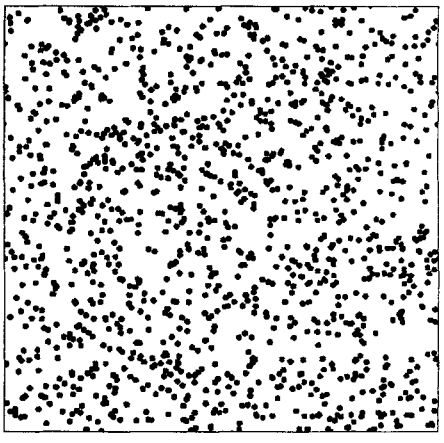

Figure 1a. Computational grid generated by randomly overlapping pores with uniform size.

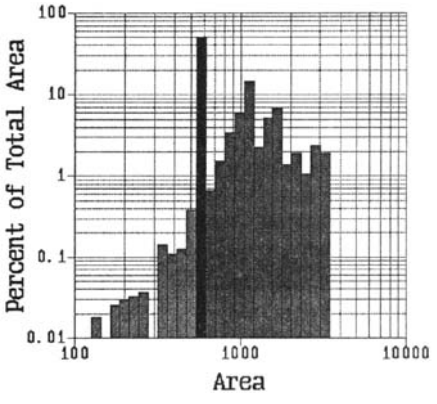

Figure 1b. Resulting pore size distribution.

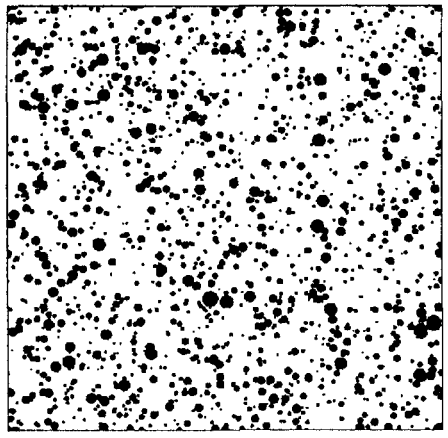

Figure 2a. Computational grid generated by randomly overlapping pores with a distribution of sizes.

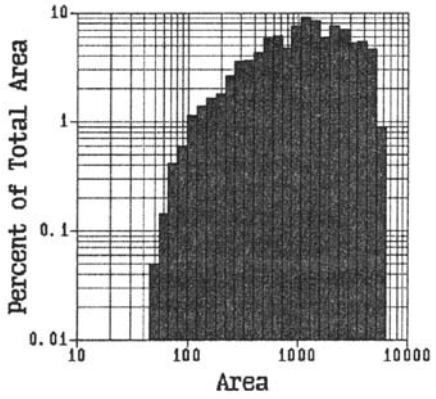

Figure 2b. Resulting pore size distribution.

the same porosity and pore surface area, yet their pore size distribution curves are substantially different, Figures 1b and 2b. Finally, the first image of Figure 3 ($x = 0.0$) displays a 1,024 × 1,024 grid generated by randomly distributing circles of two widely different sizes. The resulting bimodal pore size distribution matches the measured macropore structural properties of the same Illinois No. 6 char. Thus, one can generate computational grids modeling arbitrary pore size distributions obtained from structural measurements. Models that employ grids generated by randomly distributing on them entities of uniform size or whose size follows a unimodal density function will be referred to subsequently as *unipore* models. *Bipore* models employ grids generated by randomly distributing on them entities of two sizes (or whose size follows a bimodal distribution).

Once the grid is initialized, the entities corresponding to pores are grown according to rules simulating kinetic- or diffusion-controlled reactions. When chemical reaction controls, the entire surface area is equally accessible to the reactants and all pores will grow at the same rate. The simulation then will progress in time by reacting (or setting to black) all the solid (white) cells adjacent to pore (black) cells at each step. The computational grid is analyzed after each time step and the volume of the solid phase is obtained by counting. Thus, the conversion is immediately calculated and the pore surface area is obtained by numerical differentiation. Figure 3 highlights the evolution of the pore structure when a solid with bimodal pore

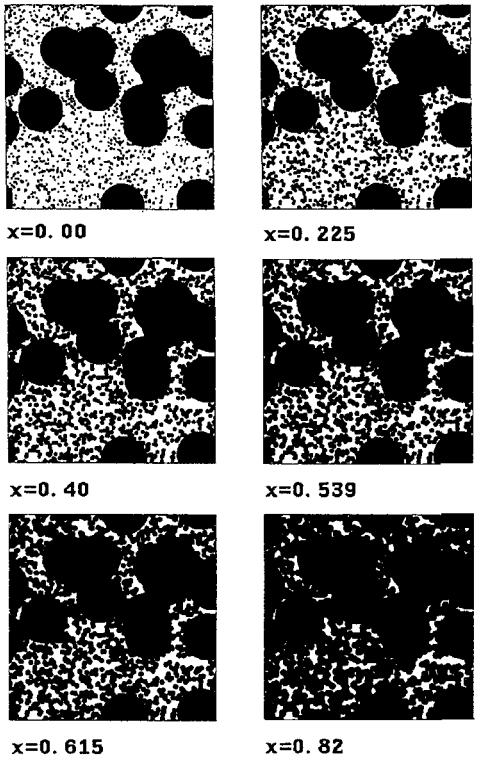

Figure 3. Image sequence computational grids from a bi-pore model at several conversion levels.
Original grid models macropore structure of an Illinois No. 6 char

size distribution reacts in the kinetic control regime. This image sequence clearly indicates that the solid will disintegrate into small fragments at conversion levels higher than 50%. The discrete modeling approach allows the use of image analysis techniques to obtain the size distribution of the overlapping pores or of the particle fragments at any conversion level.

The evolution of pore structures in the presence of intraparticle diffusional limitations is a more challenging problem. Local reaction rates can vary significantly throughout the solid particles and pore connectivity is a major factor in determining the local structural changes. Since it is impossible to ascertain the pore connectivity via direct or indirect measurements, we have concentrated on the analysis of important limiting cases. When reactions take place in the regime of strong intraparticle diffusional limitations, only the exterior surface of the particle (or a particle fragment) will be available to the gaseous reactants. In this case, only the solid cells located on the exterior surface of a particle (or of a fragment) will be reacted at every step of a discrete simulation. Finally, reactions in the regime of intermediate intraparticle diffusional limitations may be simulated by assuming that the rate of pore growth depends on their location within the particle, their size, and other factors to be discussed.

Determination of initial grid configuration

The numbers and sizes of entities distributed on the initial grid are determined by a modification of a statistical method first proposed by Ballal and Zygourakis (1987a). The main simplification introduced here involves the handling of *edge effects*. Let us consider the simple case of distributing circles (or other

two-dimensional entities corresponding to pore cross sections) on a square (i.e., on a face of the representative cube). When the distance between the center of a circle and the edge of the square is smaller than the circle radius, however, part of the cylindrical pore will be located outside the cube and the computed pore volume and surface areas must be appropriately adjusted. Treatment of such edge effects necessitated lengthy and complicated algebraic manipulations. The discrete models handle such situations in a simple fashion, making edge effect compensation unnecessary. As shown in Figure 4, when circles fall near an edge or a corner of the square simulation grid, we extend (or overlap) them onto the opposite edges according to a simple transformation.

We will now outline the development of the set of simplified nonlinear equations whose solution determines the number and size of entities that must be randomly distributed in the representative cube in order to obtain a model porous solid with given porosity and surface area. Assuming entities of equal volume V_e, the probability that a point in the cube is contained in a single entity is:

$$P_1 = \frac{V_e}{h^3} \tag{2}$$

The probability of a point not being covered by the entity is $(1 - P_1)$. If N entities are distributed upon the cube randomly, the probability P that a point is contained in at least one of the entities is:

$$Pr = 1 - (1 - P_1)^N \tag{3}$$

According to Robbin's theorem (1944, 1945), the volume of pores in the representative cube is:

$$V = h^3 [1 - (1 - P_1)^N] \tag{4}$$

All overlapping pores distributed in the cube have the same radius r. These pores will grow due to the heterogeneous chemical reactions occurring on their walls and their radius will increase. The pore volume increase dV corresponding to an increase of the radius by dr is given by

$$dV = S\, dr \tag{5}$$

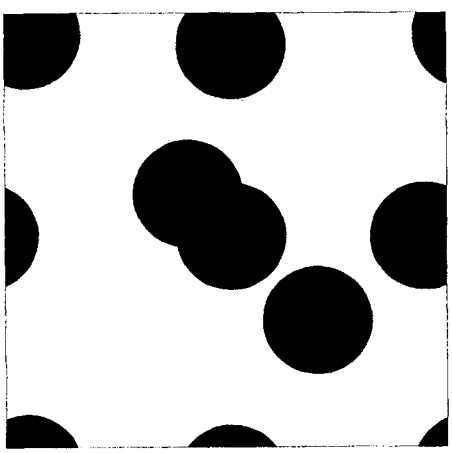

Figure 4. Simple computational grid illustrating treatment of edge effects by discrete models.

This can be stated without losing generality by viewing r as a characteristic dimension of the entities which increases as the pores grow. We can thus determine the surface area by differentiating the change in volume:

$$S = \frac{dV}{dr} = h^3 N (1 - P_1)^{(N-1)} \frac{dP_1}{dr} \tag{6}$$

If S_e is the surface area of a single entity (cylinder or sphere)

$$\left(\frac{dP_1}{dr}\right) = S_e$$

and the following dimensionless equations can be obtained to relate the population parameters N and r to measurable physical properties of the solid:

$$\epsilon = \frac{V}{h^3} = 1 - F^N \tag{7}$$

$$\beta \equiv \rho S_g h = N F^N G \tag{8}$$

$$F = \left(1 - \frac{V_e}{h^3}\right), \quad G = \frac{1}{F}\left(\frac{S_e}{h^2}\right) \tag{9}$$

where ϵ is the porosity, ρ is the bulk density, and S_g is the specific pore surface area per unit mass of the solid. As $h \to \infty$, Eqs. 7 through 9 agree with the expressions derived by Ballal and Zygourakis (1987a).

By solving the nonlinear Eqs. 7 through 9, we obtain the number N and size r of entities that must be randomly distributed on the discrete computational grid to model a porous solid with given structural properties. A congruential pseudorandom number generator (Rubinstein, 1981) is used to compute the locations of the geometrical centers of the pores, and the values of surface area and porosity obtained for each realization are computed by image analysis techniques. The parameters N and r may then be altered slightly in an iterative procedure to improve the agreement between model and experimentally measured properties. Usually the iterative procedure is continued until matches within 5% of all values are obtained.

Equations for overlapping entities of two sizes were also developed in a similar manner. In this case, we randomly distribute in the cube N_1 entities with volume equal to V_{1e} and N_2 entities with volume equal to V_{2e}, where it is assumed that $V_{2e} \gg V_{1e}$. Four nonlinear equations are thus obtained relating N_1, V_{1e}, N_2, and V_{2e} to the porosities and surface areas of the two size fractions. It is important, however, to emphasize that the treatment of edge effects adopted here greatly simplifies the equations. The expressions for the F and G functions corresponding to the four-parameter model have the simple form indicated by Eq. 9 instead of the more complicated functionality presented in an earlier communication (Ballal and Zygourakis, 1987a).

We should note that the statistical analysis predicts no difference in the expected values of structural properties when, for example, cylindrical pores are all parallel to each other or when their directions are randomly distributed in a three-dimensional domain. This implies that differences between models that assume parallel or randomly oriented pores should be small when all pores grow at the same rate.

Discrete simulations and analytical random-pore models

The largest two-dimensional computational grids used in this study contained 4,096 × 4,096 cells, while the three-dimensional simulations were run on 256 × 256 × 256 grids. Sophisticated data structures were employed to store and process information on the changing computational grids. This allowed efficient handling of even the largest computational grids used here in less than 1 Mbyte of physical memory. The simulations required from 10 min to 2 h of CPU time on a VAX 11/750 minicomputer.

A detailed error analysis was carried out (Sandmann, 1986) to establish the validity of the discrete simulation approach. Among other factors, this analysis considered:

1. The rasterization error introduced when regular geometrical objects are approximated by domains consisting of square or cubic cells
2. The effects of the randomly generated initial distributions of pores

Rasterization introduces errors in the evaluation of pore volumes at each simulation step and results in a scatter in the porosity evolution data. By using pores with radii larger than seven cell lengths, the scatter was reduced to acceptable levels. The small variations still present were smoothed by fitting the conversion data with a piecewise polynomial approximation using B-splines and smooth rate curves were obtained by differentiating the polynomial approximant.

When different seeds are used to generate the sequence of pseudorandom numbers for distributing the entities on the initial grid, different porosities and surface areas are obtained and, as a result, variations in the predicted surface area vs. conversion curves are observed. By using large computational grids (4,096 × 4,096) and large numbers of randomly distributed pores (typically 2,000 to 5,000), the maximum deviations from the average property values were reduced to below 1%. The property averages were computed from the results of several runs with the same grid size and number of pores.

Thus, only one simulation on a large grid is usually required to achieve statistically significant results for the reaction of any porous solid in the kinetic control regime. When many overlapping pores are distributed on large computational grids, the reactivity patterns obtained from the discrete models become virtually identical (as expected) to those predicted by available analytical random-pore models (Ballal and Zygourakis, 1987a). It must be emphasized, however, that the discrete models can easily treat complex pore structures and they can provide detailed structural information not obtainable with any of the available analytical models.

Effects of Various Pore Structure Parameters

Several assumptions made during the generation of initial computational grids can affect the surface area vs. conversion patterns predicted by the discrete simulations. The effects of some assumptions concerning the orientation of pores, their size distributions, and the shape of pore cross sections will be briefly considered.

The use of overlapping parallel cylindrical pores may appear at first glance to lead to an oversimplified representation of the pore structure of actual solids. In order to test this hypothesis, we carried out simulations with three-dimensional computational grids that considered:

1. Cylindrical pores oriented along three perpendicular directions parallel to the faces of the representative cube
2. Cylindrical pores with random orientations inside the cubic computational grids.

In all cases, the three-dimensional simulations produced results virtually indistinguishable from those obtained from two-dimensional simulations using parallel cylindrical pores. These results agree with the statistical analysis discussed in the previous section. Three-dimensional simulations using two populations of cylindrical and spherical pores also yielded results very similar to those obtained from two-dimensional simulations employing overlapping pores of two sizes. Two-dimensional simulations are thus adequate for modeling gas-solid reactions in the kinetic control regime and should be preferred since they are computationally more efficient.

We have also investigated the possible effects of distributing entities of nonuniform size on the initial simulation grids. As an example, the grids shown in Figures 1a and 2a were used to simulate reaction in the kinetic control regime. Note that both those grids model the micropore structure of an Illinois No. 6 char and have the same porosity and pore surface area. Figure 5 presents the surface area vs. conversion curves from the two simulations. The use of a pore size distribution in the generation of the initial grid had only minor effects on the reactivity pattern. The shape of the curve remained essentially the same, with a slightly higher maximum. Such differences are not considered significant given the uncertainties in the experimentally measured values of porosity and surface area. At this point, the use of unimodal or bimodal pore size distributions for generating the initial grid does not appear to be a significant modification of the simpler models that utilize overlapping pores of one or two uniform sizes.

We have so far assumed that pores are formed by overlapping circular cylinders (or spheres). That, however, may not be an

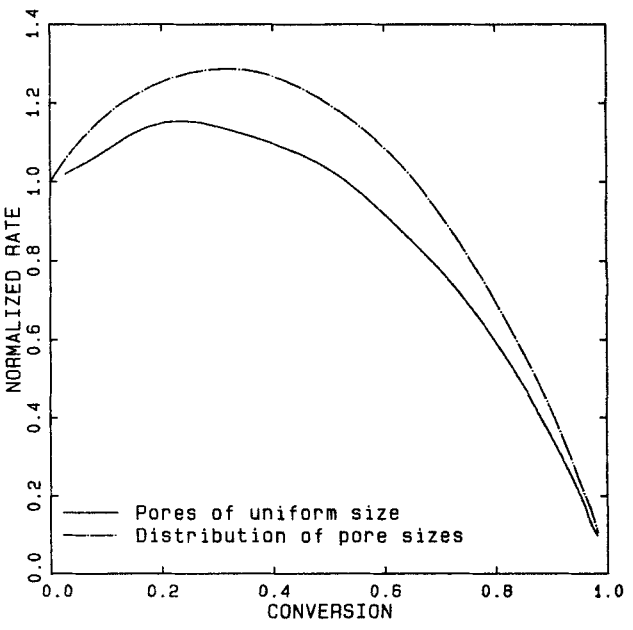

Figure 5. Effect of pore size distribution on predicted reaction rates.

accurate representation of the pore structure of actual solid reactants. In addition, overlapping pore models cannot account for the creation of new pores during reaction, a phenomenon that has been observed in some instances.

In order to model pores of highly irregular cross section, solid "grains" were randomly distributed on the initial grid. Pores were thus formed by the interstitial voids among the overlapping grains of the solid reactant. Straightforward modifications of Eqs. 2 through 9 yielded the number and size of solid grains that must be randomly distributed on a grid in order to model solids with given porosities and surface areas. Figure 6a presents such a grid obtained by randomly distributing cylindrical grains to match measured macropore properties of a lignite char studied in our laboratory. In order to simulate heterogeneous reactions occurring on the grain boundaries, the initial grid was modified by shrinking the cylindrical grains. Note that as grains erode due to reaction, new pores will appear at points where the solid grains overlap.

Figure 6b compares surface area evolution curves predicted from an overlapping grain simulation and from an overlapping cylindrical pore simulation for the same lignite char. The overlapping grain model produced a curve with a more pronounced maximum that occurred at a conversion level much higher than the one predicted by the overlapping pore model. These results show that the shape of pore cross sections and the generation of new pores can significantly affect the reactivity pattern. A similar result was obtained by Ballal and Zygourakis (1987b) for the simpler case of pore cross sections with rectangular geometry and various aspect ratios.

Effects of an Inert Solid Phase

An important feature of discrete models is that they can easily be extended to simulate the reaction of porous solids containing a second inert solid phase. Computational grids with three-state cells (pore, solid reactant, solid inert) were used to model the reaction of chars containing inorganic impurities (ash). Ash particles of uniform size were randomly distributed on the computational grid and it was assumed that they block surface area without spreading.

Figure 7 presents the surface area vs. conversion curves for the gasification of a model char containing no ash and 33% ash. As expected, the ash content caused a flattening of the curve maximum and a shift of its location toward lower conversions.

Simulations were also performed on a Texas lignite char chosen for the modeling effort because of its large ash content (40%). Several size distributions of ash particles are simulated, ranging from a large number of small ash particles to just a few large ash particles. The tested range of size distributions matched qualitatively those obtained experimentally from a scanning electron microscope study performed on the lignite char. Each of the distributions simulated produced almost identical reaction curves for the lignite char.

Application of Discrete Models to Char Gasification

The versatility and usefulness of the discrete models can best be demonstrated by employing them to analyze experimental reactivity data obtained from gasifying a variety of carbonaceous materials.

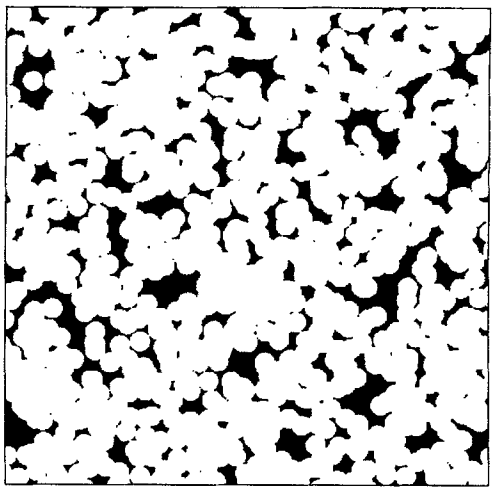

Figure 6a. Computational grid for discrete model with overlapping solid grains.

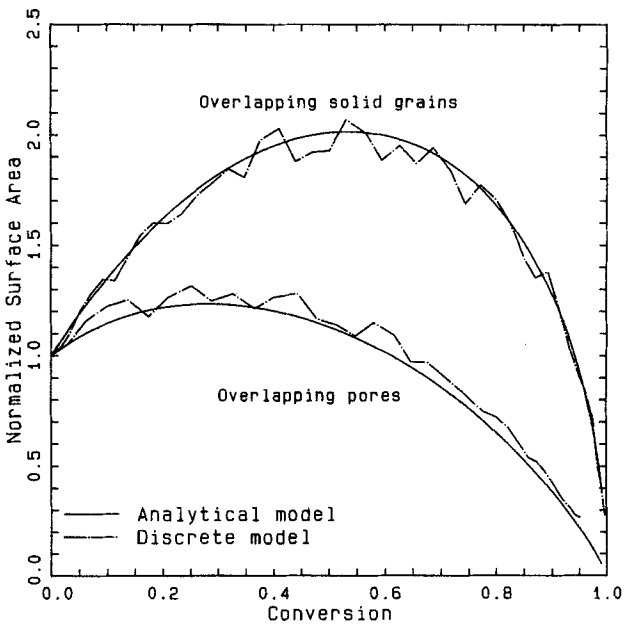

Figure 6b. Comparison of reaction rate predicted for above grid to rate obtained from a discrete model with overlapping cylindrical pores.

Solid reactants with pores of widely different sizes

Some of the coal-derived chars studied in our laboratory exhibited pores of widely different sizes (Ballal and Zygourakis, 1987b; Sandmann and Zygourakis, 1987). Pores ranged from spherical cavities with equivalent diameters as high as 200 μm for particle diameters between 400 and 500 μm, down to submicropores with diameters smaller than 0.8 nm. Structural measurements obtained for the various pore size ranges can be used to calculate the necessary parameters for the discrete models. It is impossible, however, to simulate reactions of such solids on a single computational grid. Even the largest allowed grids do not provide the spatial resolution necessary to model pores whose sizes differ by five or six orders of magnitude.

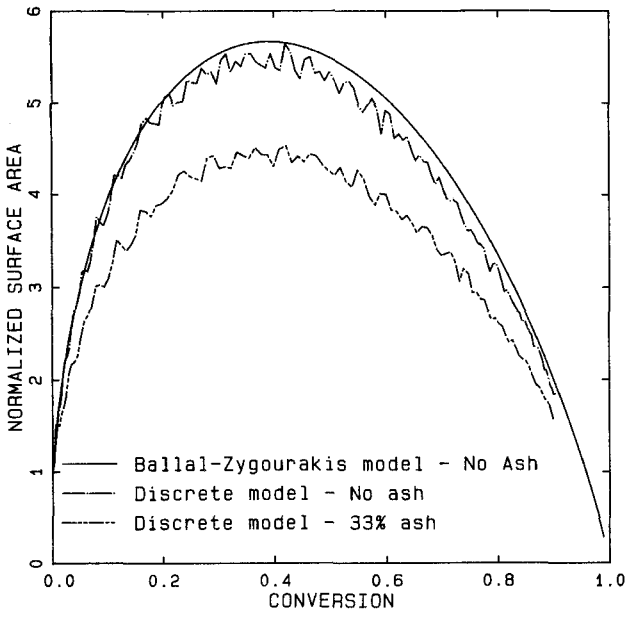

Figure 7. Effect of ash on predicted surface area evolution curves.

We use separate computational grids to simulate the reaction of the large pores (macro- or mesopores) and of the small pores (micro- and submicropores) in the kinetic control regime. The reactant phase in a macropore simulation grid, Figure 3, is treated as a microporous solid, whose properties at various conversions are calculated from a second simulation performed on a different computational grid modeling the micropore structure, Figure 1a. By interpolating the results from the two simulations at equivalent times, we obtain the overall porosity and surface area. This approach effectively models the pore structure as a network of micropores branching out from the sides of much larger macropores. Provided that time and length scales are properly matched, this approach can also be used to combine results from different models.

By combining results obtained from two or more runs on large grids, the discrete models have the ability to handle solids with pores ranging over several orders of magnitude. With two runs on separate 4,096 × 4,096 grids, for example, an effective resolution provided by 16 million cells in each direction is achieved. Thus, the number of cells used here to model complex pore structures is several ordres of magnitude greater than the number of cells (65,000) typically reported in percolation theory simulations (Mohanty et al., 1982).

We use two analytical methods to measure structural properties associated with pores in each of the two size ranges:

1. Optical microscopy for macropores with diameters over 1.0 μm and porosimetry for pores between 50 nm and 1.0 μm
2. N_2/BET and CO_2/DP adsorption for the larger micropores and the submicropores, respectively

Thus, unipore or bipore models can be used for each of the two simulations, resulting in four possible alternatives for computing the combined results. For example, a unipore model with parameters obtained from optical microscopy measurements can be used to simulate reaction in the macropore structure, while a bipore model can be used to simulate reaction in the smaller pores. In the latter case, pores of two uniform sizes are distributed on the second simulation grid to match the micropore and submicropore properties obtained from N_2/BET and CO_2/DP adsorption data. A parametric study (Sandmann and Zygourakis, 1986) established that significantly different model predictions are obtained from the various alternatives available for modeling reaction in the kinetic control regime (i.e., a single simulation for the micropores or one of the four possible double-simulation combinations). In the kinetic control regime, the structural properties of the micro- and submicropores as well as the total porosity of the solid are the most important factors determining the surface area evolution pattern. The macropore structural properties, however, become important in the presence of intraparticle diffusional limitations. Good characterization of the pore structure is thus essential for accurate model predictions.

Incomplete pore utilization

The discrete models can easily handle incomplete pore utilization that occurs in the intermediate reaction regime where both chemical kinetics and pore diffusion make comparable contributions to the overall rate. In order to model incomplete utilization of the submicropores of a char, for example, the smaller pores may be grown at slower rates than those used for the larger pores. Clearly, the ratio of these two growth rates provides a measure for the degree of utilization η of the submicropores. A simple parametric study based on varying the ratio of pore growth rates was used by Sandmann and Zygourakis (1987) to interpret an interesting reactivity behavior that was caused by incomplete utilization of the smaller micropores.

More realistic situations can also be treated easily by the discrete models. For example, the growth rates of pores can be considered to be functions of their spatial position, and diffusional limitations can thus be modeled by decreasing the pore growth rate with increasing distance of the pore center from the particle exterior. Figure 8 presents model predictions from simulations that assumed first-order reaction with diffusional limitations in a porous slab of solid reactant. Increased values of the Thiele modulus φ were accompanied by sharper decreases in the growth rate of pores located in the particle interior. For intermediate values of φ, the reactivity curve exhibits an inflection point after the observed maximum. Such inflection points appeared in several of our experimental char reactivity curves when the gasification temperature was raised above a certain level (Sandmann and Zygourakis, 1987). Inflection points in the char reactivity curves were not observed at the lower temperatures used in our studies for each char/gas pair.

These are two simple examples demonstrating the flexibility of the discrete models. One can easily vary the growth rate of pores as a function of both size and distance from the particle exterior. Also, the dependence of effective diffusivities and pore growth rates on local conversions can easily be incorporated into the discrete models, since we can easily compute the local porosity at various regions of the computational grid. Such computations are made possible by image analysis techniques that allow us to isolate and analyze any region of the computational grid.

Partially ordered pore structure

Figure 9b shows the reactivity pattern obtained by gasifying an activated carbon with CO_2 (Sandmann and Zygourakis, 1987). This pattern shows a sharp initial maximum followed by a plateau where the gasification rate changes little over a considerable range of conversions. We could not adequately simulate

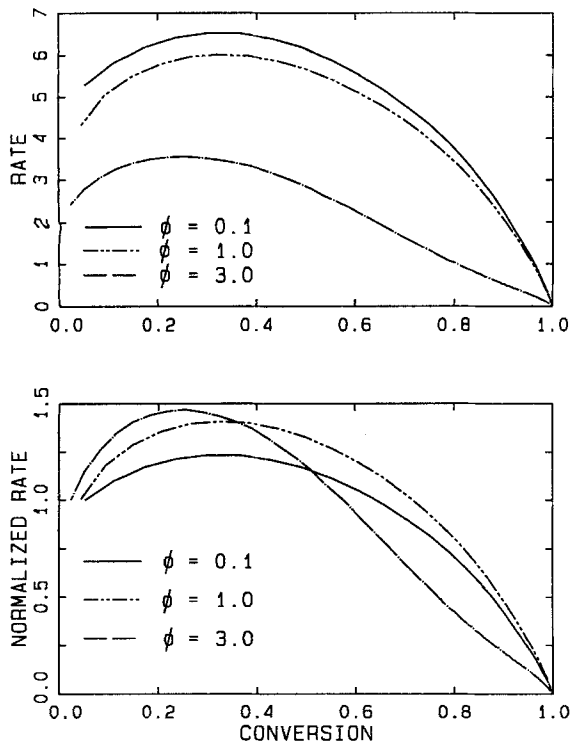

Figure 8. Predicted effects of diffusional limitations in the micropores on reactivity pattern of the Illinois No. 6 char.

this reactivity curve with any of the variants of random-pore models. However, the high reactivity of this material at conversions above 90% strongly indicated the presence of an ordered pore structure. Partially ordered pore structures have been reported for heat-treated carbonaceous materials (Monthioux et al., 1982; Joseph and Oberlin, 1983; Dubinin, 1982) and are consistent with mechanisms involving the appearance of a liquid crystalline phase (carbonaceous mesophase) during the pyrolysis stage (Brooks and Taylor, 1968). Liquid crystalline regions are formed due to a partial ordering of planar fused-ring macromolecules produced by the aromatic condensation reactions occurring during pyrolysis. These observations imply that the addition of some order to a fraction of the smallest pores might produce structures modeling more closely the actual porous solids. A computational grid modeling a partially ordered pore structure is shown in Figure 9a. The ordered pores in this particular example were generated from the CO_2/DP adsorption data for the activated carbon. Structural properties obtained from N_2/BET adsorption data were used to superimpose a network of larger randomly distributed pores on the computational grid. Simulations with such partially ordered pore structures yielded predictions providing good fits to the experimental gasification data for the activated carbon as shown in Figure 9b. This agreement indicates that partially ordered pore models may provide a reasonable approximation to the microstructure of the activated carbon (Sandmann and Zygourakis, 1987).

It must be noted here that discrete simulations with completely ordered pore structures (Sandmann and Zygourakis, 1986) produced surface area evolution patterns exhibiting inflection points, sharp maxima, and large constant area regions or initial steep decreases in surface area. None of the available

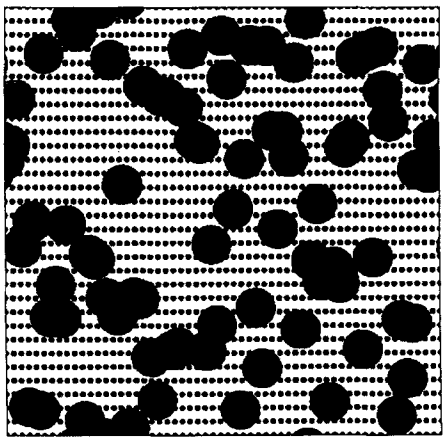

Figure 9a. Computational grid with partially ordered pore structure.

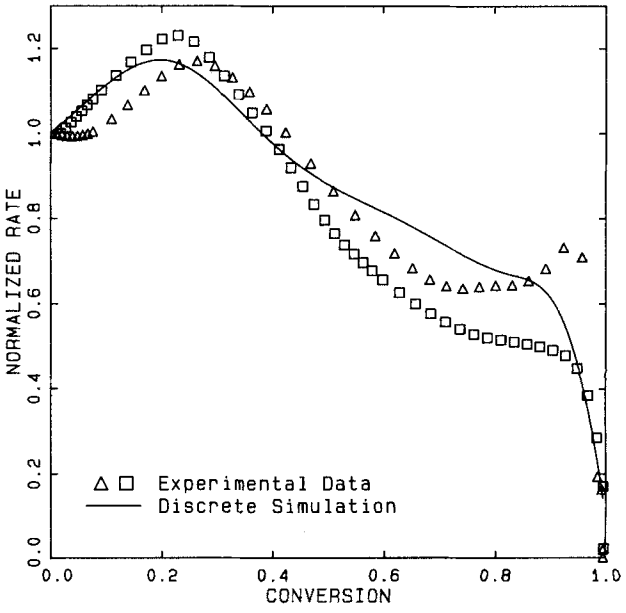

Figure 9b. Comparison of reaction rate predicted for above grid to experimental gasification data for an activated carbon.

random-pore models (discrete or analytical) can predict such a variety of reactivity patterns.

Reaction in the regime of strong diffusional limitations

Several gasification processes involve rapid coal combustion at high temperatures. Strong intraparticle diffusional limitations are present under these conditions and the surface area associated with the micro- and submicropores will not be utilized. Since most of the reacting surface will now be on the outside of the particle, a shrinking-core model could be used to simulate the gasification reaction. Such a model, however, does not take into account the irregular macropore structure of the char, the opening of initially closed porosity, and particle fragmentation. Fragmentation phenomena affect significantly the distribution of particle sizes during gasification and may result in substantial weight loss of carbon material. Kerstein and Niksa (1984) used a percolation model to study the fragmenta-

tion of electro- and reactor graphite materials during reaction in the kinetic control regime. Different fragmentation behavior, however, might be expected during the reaction of char particles with large internal cavities in the regime of strong intraparticle diffusional limitations.

The discrete model was used to investigate how strong intraparticle diffusional resistances affect the reaction rate and particle fragmentation. These simulations considered reaction in the macropores only and assumed that all the surface area in pores open to the particle exterior was equally accessible to the gaseous reactant. At each step of the discrete simulation, a solid cell would react only if it were located either on the exterior surface of a particle or on the surface of an open pore. The assumption of no diffusional limitations in the open pores is a reasonable approximation for many of our gas-solid systems given the large size of internal cavities observed in the char particles.

Results from two simulations on two-dimensional grids using the macropore data from the Illinois No. 6 char are shown in Figures 10 through 12. These simulations do not account for pore opening events triggered by reaction at planes parallel to the one considered. Thus, the reaction rates may be underestimated, especially at the later stages of gasification. Mercury porosimetry data were used to generate a unimodal pore size distribution for the first run; an image sequence showing the computational grids for this unipore simulation at several conversions is presented in Figure 10. Significant ablation is evident as numerous fines fragment away from the main particle core, and the predicted reaction rate, Figure 12, is much higher than that obtained from the shrinking-core model.

Data obtained from both optical microscopy and mercury porosimetry were employed to generate a bimodal pore size distribution for the second run, Figure 11. This simulation explained the large internal vesicles not properly measured by porosimetry; the grids corresponding to several conversion levels are shown in Figure 12. One can immediately observe:

1. Reaction rates are now lower than those predicted by the unipore simulation, Figure 12, due to the redistribution of porosity to larger pores
2. The reaction rate increases sharply when the reaction front reaches the large internal cavities previously unavailable for reaction
3. The particle now fragments into pieces of several large sizes in addition to the fines

It should be noted that rate predictions from the bipore model are strikingly similar to experimental reactivity data obtained by gasifying single coal particles in a fluidized bed (Sundback et al., 1984). Shrinking-core models predict combustion rates that decrease monotonically with conversion. The experimental measurements, however, revealed that combustion rates increased initially in a stepwise fashion with periodic jumps, and distinct maxima were observed for many particles. This behavior was attributed to particle fragmentation and agrees qualitatively with predictions from our discrete models. Unfortunately, however, detailed pore structural data for these char particles were not presented.

These results clearly indicate that the macropore structure controls the reactivity behavior. Even the largest grids used for bipore simulations, however, can have only a small number of large cavities. Thus, several simulations with different initial distributions of pores must be averaged to obtain the expected overall rate in the regime of strong diffusional limitations. The average rate computed from nine simulations with different initial grids is shown in Figure 12 for the case of bimodal macro-

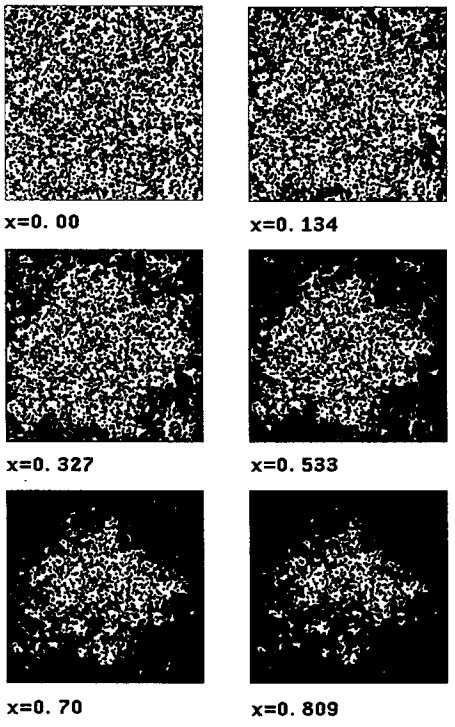

Figure 10. Strong intraparticle diffusional limitations.
Image sequence showing computational grids from a unipore model at several conversion levels. Illinois No. 6 char; macropore properties from mercury porosimetry data

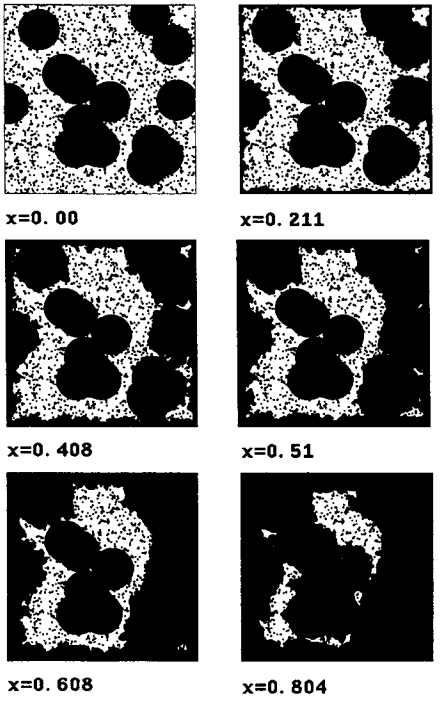

Figure 11. Strong intraparticle diffusional limitations.
Image sequence showing computational grids from a bipore model at several conversion levels. Illinois No. 6 char; macropore properties from optical microscopy and mercury porosimetry data

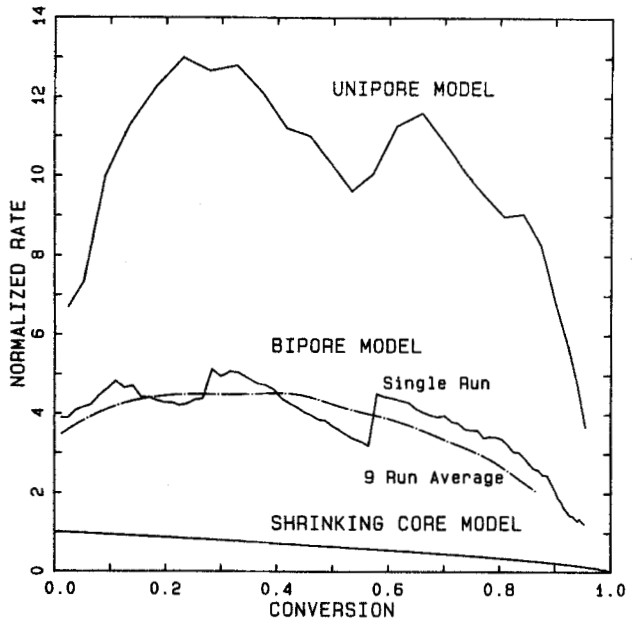

Figure 12. Predicted reactivity patterns for gasification in regime of strong intraparticle diffusional limitations.
Illinois No. 6 char

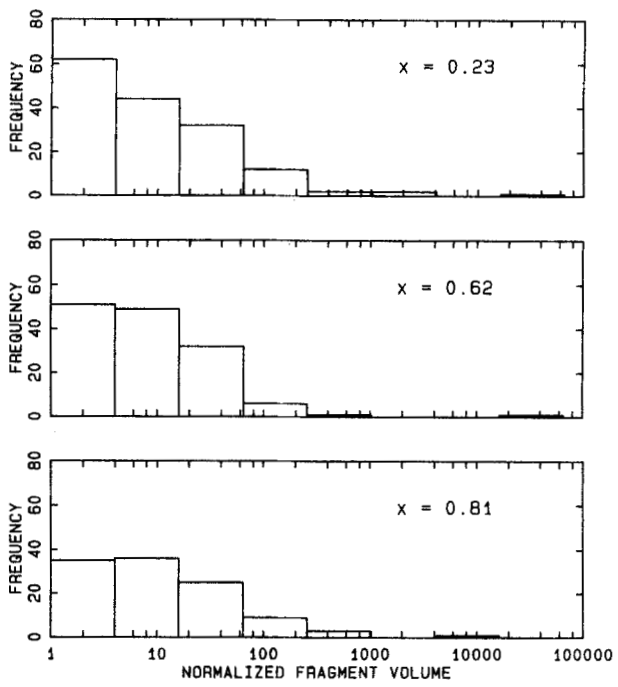

Figure 13. Number frequency of particle fragments at various levels of conversion from a unipore model simulating reaction in regime of strong intraparticle diffusional limitations.
Illinois No. 6 char; macropore properties from mercury porosimetry data

pore size distributions. Averaging has eliminated the sudden jumps present in results from a single simulation and the smooth curve is the expected behavior predicted for this char sample.

Using digital image processing techniques, computational grids at various levels of conversion were analyzed to obtain particle fragmentation data. By processing the grids displayed in Figures 10 and 11, histograms of the number frequency of fragments vs. their size were obtained; they are shown in Figures 13 and 14. The distribution giving the total volume of fragments falling in a particular size range can also be obtained easily. The important thing to notice here, however, is the different fragmentation behavior observed in simulations with different macropore structures. A large number of fines is produced when the solid exhibits a narrow distribution of small macropores, indicating possible significant weight loss during gasification. When most of the pore volume is attributed to large internal cavities, on the other hand, the particle fragments into pieces of several large sizes and a smaller amount of fines is produced.

The large difference in the rate and fragmentation results obtained with the unipore and bipore models indicates that good macropore characterization is essential for accurate predictions of gasification behavior in the regime of strong intraparticle diffusional limitations. Initial grids for simulations could be obtained from digitized photomicrographs of polished char samples.

Simulations using two-dimensional grids are not sufficient to accurately model gasification of actual solids in the regime of strong intraparticle diffusional limitations. Three-dimensional grids were also used to simulate reaction under these conditions, but memory limitations restricted their size to a maximum dimension of 256 × 256 × 256 cells, producing less accurate results. The complex connectivity of three-dimensional pore networks increased the computation time for such simulations. Preliminary results revealed behavior similar to that observed in the two-dimensional cases with lower maxima. The greater connectivity of the three-dimensional sample resulted in less particle fragmentation. All the possible pore growth patterns were not considered in our preliminary models, however, and more sophisticated models are currently being developed. It may also be possible to modify two-dimensional results with appropriate correction factors in order to obtain accurate reactivity and fragmentation results using only a fraction of the computations required for simulations with three-dimensional grids.

Conclusions

The discrete models described here provide a powerful tool for investigating gas-solid reactions. Direct observation of the sequence of computational grids allows for visualization and better understanding of the reaction phenomena, while image processing of these grids can provide information not easily obtainable from other analytical models. Parametric studies and an error analysis validated the discrete models and established that the direct simulation approach can provide an accurate approximation to the solution of random-pore model equations for systems with arbitrary geometries or complex pore growth rules. Accurate characterization of the micropores is essential for analyzing and predicting gasification behavior in the kinetic control regime while, as expected, the macropore structure introduces only secondary effects in this case. The simulations employing grids with ordered pore arrangements strongly indicate that random-pore models may be too limited to adequately explain all the available experimental data. Ordered pore structures and changing surface activity are two essential features that must be incorporated in accurate predictive models.

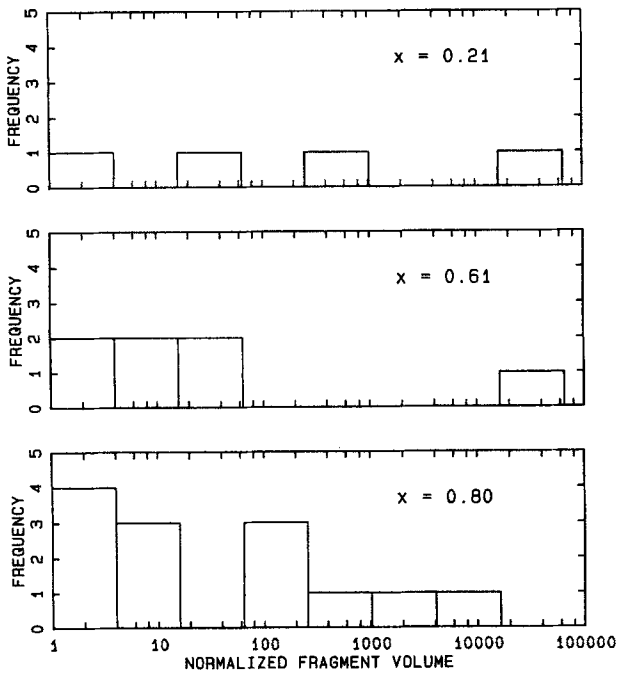

Figure 14. Number frequency of particle fragments at various levels of conversion from a bipore model simulating reaction in regime of strong intraparticle diffusional limitations.

Illinois No. 6 char; macropore properties from optical microscopy and mercury porosimetry data

Another important advantage of the discrete models lies in their ability to simulate reaction in the regime of strong diffusional limitations. Although employing a simplistic view of reaction phenomena in this regime, these models yield predictions that agree qualitatively with experimental observations. Significant particle fragmentation and attrition are predicted and they are accompanied by enhanced reaction rates and rate curves exhibiting maxima. The reactivity patterns are a strong function of the macropore structure, indicating that accurate characterization of the macropores via a combination of analytical techniques is necessary.

The direct simulation approach presented here can be applied to a variety of phase-growing or gas-solid reacting systems. Computational grids are not limited to square or cubic lattices. Polyhedric or other lattices could be used if that were considered necessary. Systems with two or more reacting and/or inert phases can also be simulated using cells with the appropriate number of states. In a simple example of such simulations, cells with three states were employed to model the reaction of a porous char containing inert inorganic impurities. More complex pore growth rules can also be employed to simulate other noncatalytic or catalytic systems.

Notation

$A(x)$ = active fraction of total pore surface area
F, G = functions, Eq. 9
h = length of side of representative cube, m
N = number of overlapping pores
r = characteristic size (radius) of a pore, m
R = reaction rate, s^{-1}
S = total pore surface area of overlapping pores, m^2
S_e = surface area of a single geometrical entity, m^2
S_g = specific pore surface area of solid, m^2/g
V = total volume of overlapping pores in representative cube, m^3
V_e = volume of a single geometrical entity, m^3
x = conversion of solid reactant

Greek letters

ϵ = porosity of solid
η = utilization factor for pores
ρ = bulk density of porous solid particle, kg/m^3

Literature Cited

Ballal, G., and K. Zygourakis, "Evolution of Pore Surface Area During Noncatalytic Gas-Solid Reactions. I: Model Development," *Ind. Eng. Chem. Res.*, **26,** 911 (1987a).

———, "Evolution of Pore Surface Area During Noncatalytic Gas-Solid Reactions. II: Experimental Results and Model Validation," *Ind. Eng. Chem. Res.*, **26,** 1787 (1987b).

Bhatia, S. K., and D. D. Perlmutter, "A Random-Pore Model for Fluid-Solid Reactions. I: Isothermal, Kinetic Control," *AIChE J.*, **26,** 379 (1980).

———, "A Random-Pore Model for Fluid-Solid Reactions. II: Diffusion and Transport Effects," *AIChE J.*, **27,** 226 (1981).

Brooks, J. D., and G. H. Taylor, "The Formation of Some Graphitizing Carbons," *Chemistry and Physics of Carbon,* P. L. Walker, P. A. Thrower, eds., Dekker, New York, **4,** 243 (1968).

Dubinin, M. M., "Microporous Structures of Carbonaceous Adsorbents," *Carbon,* **20,** 195 (1982).

Gavalas, G. R., "A Random Capillary Model with Application to Char Gasification at Chemically Controlled Rates," *AIChE J.*, **26,** 577 (1980).

Joseph, D., and A. Oberlin, "Oxidation of Carbonaceous Matter. II: X-ray Diffraction and Electron Transmission Microscopy," *Carbon,* **21,** 565 (1983).

Kerstein, A. R., and S. Niksa, "Fragmentation During Carbon Conversion: Predictions and Measurements," *20th Int. Symp. on Combustion,* Ann Arbor, MI, 941 (Aug., 1984).

Mohanty, K. K., J. M. Ottino, and H. T. Davis, "Reaction and Transport in Disordered Composite Media: Introduction of Percolation Concepts," *Chem. Eng. Sci.*, **37,** 905 (1982).

Monthioux, M., M. Oberlin, A. Oberlin, X. Bourrat, and R. Boulet, "Heavy Petroleum Products: Microstructure and Ability to Graphitize," *Carbon,* **20,** 167 (1982).

Robbins, H. E., "On the Measure of a Random Set. I." *Ann. Math. Stat.*, **15,** 70 (1944).

———, "On the Measure of a Random Set. II." *Ann. Math. Stat.*, 16, 342 (1945).

Rubinstein, R. Y., *Simulation and the Monte Carlo Method,* Wiley, New York (1981).

Sandmann, C. W., Jr., "Fundamental Studies on Gas-Solid Reactions: Pore Structure and Reactivity of Coal Chars," Ph.D. Diss., Rice Univ., Houston, TX (1986).

Sandmann, Jr., C. W., and K. Zygourakis, "Evolution of Pore Structure During Gas-Solid Reactions: Discrete Models," *Chem. Eng. Sci.*, **41,** 733 (1986).

———, "Pore Structure Evolution During Noncatalytic Gas-Solid Reactions. IV: Studies with Demineralized Chars," *Chem. Eng. Commun.*, **58,** 139 (1987).

Su, J. L., and D. D. Perlmutter, "Effect of Pore Structure on Char Oxidation Kinetics," *AIChE J.*, **31,** 973 (1985).

Sundback, C. A., J. M. Beer, and A. F. Sarofim, "Fragmentation Behavior of Single Coal Particles in a Fluidized Bed," *20th Int. Symp. on Combustion,* Ann Arbor, MI, 1495 (Aug., 1984).

Manuscript received Feb. 18, 1987, and revision received July 18, 1988.